Available online at www.sciencedirect.com
ScienceDirect
Journal of the European Ceramic Society 30 (2010) 3117–3123
www.elsevier.com/locate/jeurceramsoc

Contribution to the understanding of the relationship between mechanical and dielectric strengths of Alumina

David Malec [a,*], Vincent Bley [a], Fatiha Talbi [b], Fadila Lalam [b]

[a] University of Toulouse, Laplace Laboratory, UPS, INPT, CNRS, Toulouse, France
[b] Quantum Chemistry and Physics Laboratory, M. Mammery University, Tizi-Ouzou, Algeria

Received 15 October 2009; received in revised form 2 July 2010; accepted 16 July 2010

Abstract

The experimental evolutions of the Alumina dielectric strength versus thickness (127 μm to 2.54 mm), purity (92%, 96% and 99.5%) and crystallography (single or polycrystal) have been investigated. In order to find crucial information about the mechanism responsible for the dielectric breakdown, optical and scanning electron micrograph observations have also been performed. Each breakdown channel was found to be terminated by a crater from which matter has been extracted during the breakdown process. Investigations have been focused on the breakdown path, on the evolution of the crater size versus sample thickness and on the location of molten matter after breakdown. The results tend to confirm that the dielectric breakdown of Alumina is probably originated from a mechanical failure induced by electromechanical forces acting during the voltage application.

Keywords: B. Failure analysis; C. Dielectric properties; D. Al_2O_3; E. Insulators; Toughness

1. Introduction

Since the past forty years, the knowledge of ceramic structure and its associated properties have been largely studied, at least as much as that of polymers. Among them and due to its outstanding properties such as thermal (high thermal stability, good thermal conduction), mechanical (high resistance to abrasion, high hardness), electrical (low electrical losses, low electrical conduction, high dielectric strength) and a relatively moderate price, Alumina is being used in significant applications. In spite of these many attractive properties, one of the primary drawback is its brittle nature, characterized by a low fracture toughness. Indeed, Alumina is considered as a brittle solid, i.e. cracks of atomic sharpness propagate essentially by bond rupture. Numerous works have suggested that the dielectric properties of Alumina may be closely related to its mechanical ones. The physical model which seems to be the most valuable to explain the dielectric breakdown of Alumina is an electromechanical one. However, the dielectric strength of such material is not yet well understood. The dielectric breakdown mechanism occurring in an electrical insulator has to be considered as a succession of different events. Complementary investigations are consequently necessary to confirm if the mechanical failure of Alumina may be really considered as the first stage of this multi-breakdown process.

The goal of this paper is to provide new information about the dielectric breakdown mechanism of Alumina. After a brief description of the experimental setup for dielectric breakdown measurement, the experimental results of dielectric strength versus thickness and purity will be presented. Then broken samples will be carefully observed by both microscope and Scanning Electron Micrograph to find crucial information about the dielectric breakdown process.

2. Experimental

2.1. Materials under study

The dielectric breakdown of polycrystalline α-Alumina samples having different purities (92%, 96% and 99.5%) and different thicknesses (127 μm to 2.54 mm) has been investigated in this study. Laser Induced Breakdown Spectroscopy (LIBS)[1]

* Corresponding author. Tel.: +33 561556260; fax: +33 561556452.
E-mail address: david.malec@laplace.univ-tlse.fr (D. Malec).

0955-2219/$ – see front matter © 2010 Elsevier Ltd. All rights reserved.
doi:10.1016/j.jeurceramsoc.2010.07.024

Table 1
wt% content of impurities (635 μm-thick Alumina samples).

92%	96%	99.5%
Mn: 1.61	Si: 1.10	B: 0.18
Si: 1.10	B: 0.86	Mg: 0.16
Fe: 1.06	Mg: 0.47	Ca: 0.15
Ti: 1.00	Ca: 0.21	Si: 0.13
B: 0.82	Na: 800 ppm	Fe: 400 ppm
Ca: 0.30	Fe: 290 ppm	Na: 300 ppm
Na: 0.12	Ti: 38 ppm	Ba: 90 ppm
Mg: 425 ppm	Ba: 30 ppm	Y : 45 ppm
Ba: 180 ppm	Zr: 20 ppm	Cr: 40 ppm
Cr: 150 ppm	Y: 20 ppm	Mn: 20 ppm
Zr: 60 ppm	Cr: 20 ppm	Ti: <20 ppm
Y: 30 ppm	Mn: <20 ppm	Zr: <20 ppm

has been used to estimate both nature and content of impurities (Table 1). Other structural characteristics of Alumina under test have been summarized in Table 2.

Since the dielectric breakdown of polycrystalline Alumina depends on its grain dimensions,[2] samples have been chosen with approximatively the same mean grain size.

All the samples have been tested as received (i.e. without any thermal or mechanical treatment). Initial Alumina substrates have been cut into samples having a section of 1 in. in order to be tested in the measuring cell described in the next section.

2.2. Experimental setup

The experimental setup used for the dielectric breakdown measurements is classically composed of a high voltage transformer driven by a motorized autotransformer. A current probe detects any dielectric breakdown occurring in the sample in order to switch-off the high voltage (current threshold: 10 mA rms).

The measuring cell is detailed in Fig. 1. The first electrode is plane (diameter: 15 mm) while the second one may be either the same plane electrode or a half-spherical electrode with a calibrated small radius (0.6 μm). These electrodes are stainless steel. This electrodes system is immersed in insulating perfluorinated liquid in order to prevent any flashover or partial discharges (PD) on the sample surface. This has been verified for samples having thicknesses lower than 2.54 mm. For thicker samples, the resulting breakdown is probably modified by the PD occurring in between the spherical electrode and the sample surface.

All the measurements have been performed at room temperature (RT: 20 °C).

Table 2
Main characteristics of Alumina under test.

Alumina content (wt%)	92	96	99.5
Colour	Black	White	White
Roughness Ra (nm)	475	300	325
Mean grain size (μm)	3–7	4–7	2–5
Density (g/cm^3)	3.72	3.75	3.90
Flexural strength (MPa)	365	400	440
Elastic modulus Y (GPa)	310	331	379
Compressive strength (MPa)	2380	2520	2600
Fracture toughness (MPa m$^{1/2}$)	3.05	3.98	4.9
CTE (25–200 °C) 10^{-6}/°C	6.4	6.4	6.4
Thermal conductivity (W/m K) at 20 °C	13	26	31
Relative permittivity	10.5	9.5	10

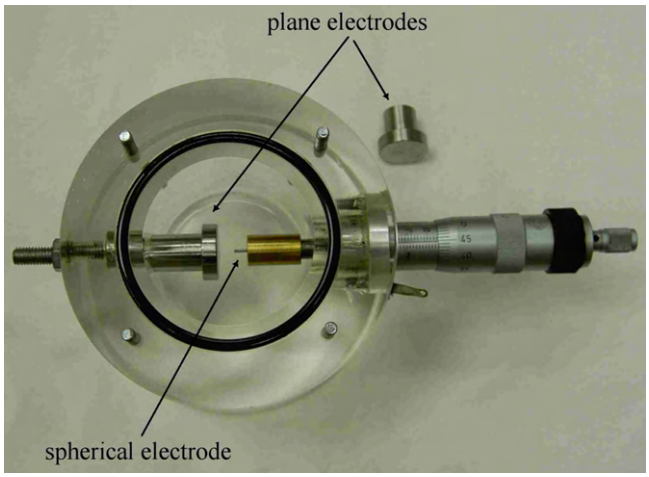

Fig. 1. Dielectric breakdown measuring cell.

3. Results

3.1. Experimental results of breakdown strength

The experimental results of dielectric strength obtained with a plane–spherical system of electrodes are reported in Figs. 2 and 3. These results are statistical values obtained from 20 different breakdowns (two samples per breakdown value) according to IEEE Std-930. Results were analyzed by the two parameters Weibull's distribution. For each breakdown value, the corresponding 90% confidence bonds have been plotted. Since a plane–spherical electrodes system has been used, the breakdown field done is a sort of 'apparent field' (volt-

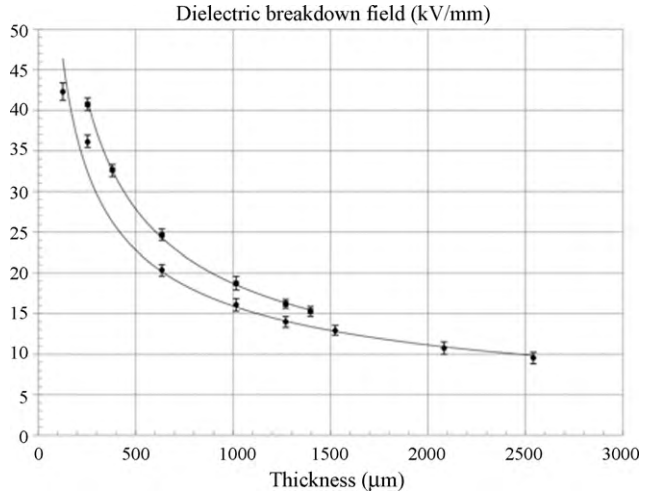

Fig. 2. Dielectric strength (rms, RT, sine 50 Hz, $\partial V/\partial t = 1.6$ kV/s) of polycrystalline Alumina samples versus thickness. Lower curve: 96% purity; upper curve: 99.5% purity.

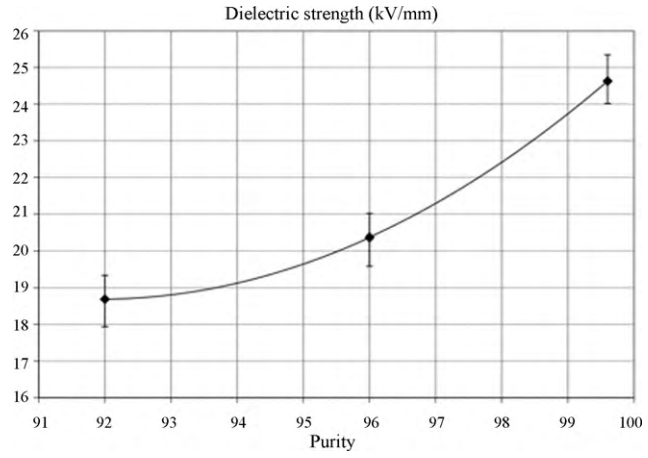

Fig. 3. Dielectric strength of 635 μm-thick polycrystalline Alumina samples versus purity (rms, RT, sine 50 Hz; $\partial V/\partial t = 1.6$ kV/s).

age/thickness) because the electrical field distribution in the sample is not uniform.

As expected,[3–6] the electrical breakdown field (E_b) of Alumina is strongly dependent on the sample thickness (d) and follows the well known relationship:

$$E_b = Ad^{-n}$$

The fit analysis of Fig. 2 leads to the following expressions (field in kV/mm and thickness in μm):

$$\text{Alumina } 96\% : E_b = 569d^{-0.51}$$

$$\text{Alumina } 99.5\% : E_b = 992d^{-0.57}$$

Both A and n parameters are found to be purity dependent.

Fig. 3 indicates that the electrical breakdown field is also dependent on the purity: the higher the purity, the higher the breakdown field.

3.2. Optical and SEM observations

All the breakdown channels have been inspected using a microscope. Irregular breakdown channels have been observed and each one is terminated by a 'crater' at the surface of the sample (Figs. 4 and 5). These observations are in good agreement with previous works.[4,7,8] A statistical analysis has shown that the size of the crater is much more important on one of the

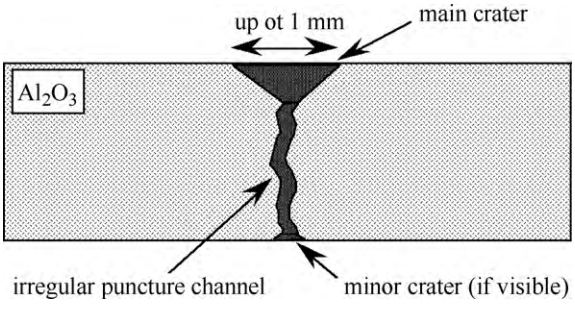

Fig. 4. Schematic structure of a dielectric breakdown channel.

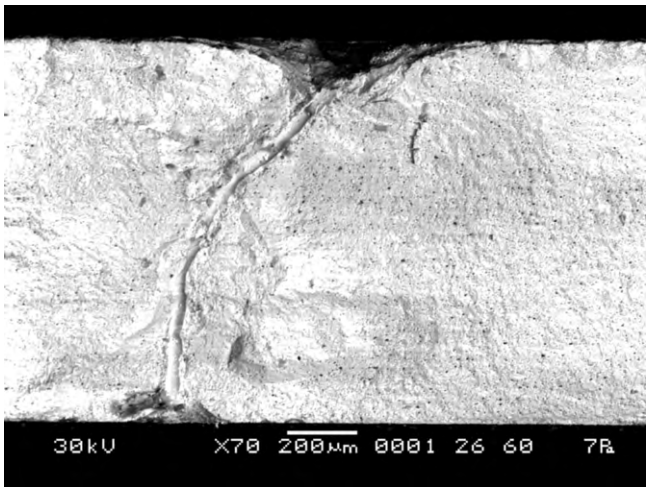

Fig. 5. Cross-section of a dielectric breakdown channel of a 1.016 mm-thick 96% polycrystalline Alumina sample (Scanning Electron Micrograph).

channel terminations.[5] On most of the samples, only one crater can be distinguished (i.e. the second crater do not exist or has dimensions close to the puncture channel ones). For plane–plane electrodes, this larger crater is located indifferently on either one surface or on the other one, while for cylindrical–plane electrodes, it is always located at the point where the half-spherical electrode is touching the sample surface.[5] These results demonstrate that the bigger crater takes place on the electrode where the interface field is the higher (plane–spherical electrodes) or where an initiating defect may be found (plane–plane electrodes).

This crater is obviously related to the breakdown (or pre-breakdown) process. Indeed, even if some voids exist in between the surface of the ceramic and the electrodes, the energy of partial discharges which may occur during the AC ramp application is not sufficiently high to create such a damage. Moreover, as the samples to be tested are immersed in a high electrical insulating liquid, the probability for partial discharges to occur is low, especially for the thin specimen broken at the lowest voltages where craters are however visible.

To verify whether the energy stored in both power supply and high voltage cable and released during breakdown is not responsible of this crater, a resistor with a high value (50 MΩ) has been introduced between the half-spherical electrode and the high voltage cable. We have then verified that, even if the current originated from the power supply is strongly limited during the breakdown process, a crater is however observed. These craters are consequently due to an event occurring during the breakdown process inside the sample and not induced by the release of any external stored energy. A meticulous observation of numerous craters has revealed that internal mechanical forces (betrayed by cracks: see the arrows in Fig. 6) are responsible of such matter ejection from the sample. In the example of Fig. 6, a part of the stressed matter has been able to withstand such mechanical forces and consequently only a part of it has been extracted from the sample.

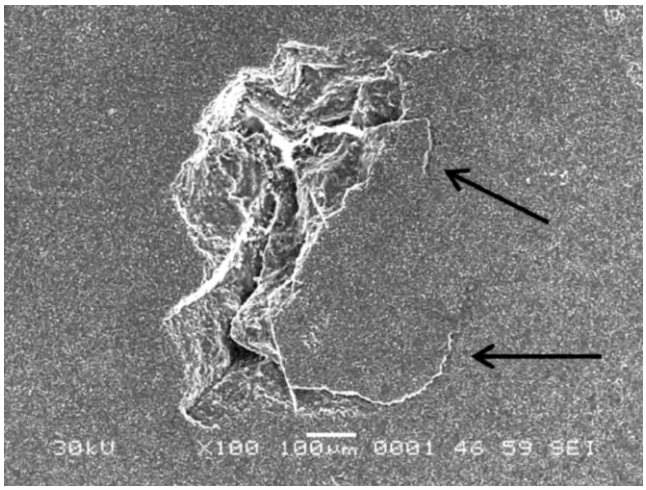

Fig. 6. Upside view of a crater partially emptied on a 1.016 mm-thick 96% Alumina sample (Scanning Electron Micrograph).

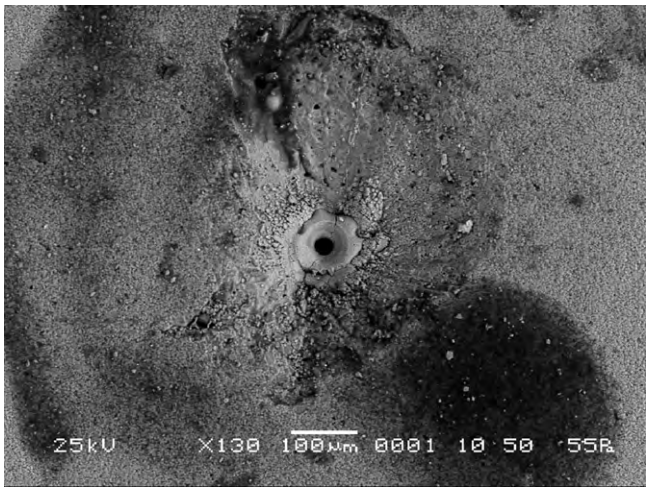

Fig. 7. Molten matter expulsed from the dielectric breakdown channel and observable at the rim of the crater of a 1.016 mm-thick polycrystalline Alumina sample (Scanning Electron Micrograph).

4. Discussion

4.1. General considerations

Optical observations of post-mortem polycrystalline Alumina samples detailed in the next section indicate that mechanical forces occur just before or during the dielectric breakdown process. The mechanical origin of the dielectric breakdown of Alumina may naturally be suggested. Electromechanical forces acting in the sample during the voltage application would lead to the propagation of a crack, following an explosive event. The toughness (ability of a material containing cracks to resist to fracture) of polycrystalline Alumina has been found to be directly related to its dielectric strength (see Table 2 and Fig. 3): the higher the toughness (i.e. the higher the purity), the higher the dielectric strength. In such hypothesis, polycrystalline Alumina should exhibit an intergranular fracture, whereas in single crystal Alumina (i.e. Sapphire) the fracture should propagate along favoured cleavage planes.[9] Indeed, in a polycrystalline ceramic the grains are crystallographically misoriented with respect to their neighbours. The grain boundaries are especially weak because of the stringent directionality and charge requirements of covalent-ionic bonds. Consequently, there is a strong probability for cracks to propagate around instead of through grains. On the contrary, for single crystal showing cleavage tendencies, a crack propagates through one cleavage plane or several cleavage planes linked by cleavage steps. Observations done on both polycrystalline and single crystal Alumina samples confirm this hypothesis. In polycrystalline Alumina, it is obviously not possible to visualize the crack path in grain boundary because of local melting and flow of matter to form the breakdown channel. Nevertheless, dielectric breakdown channels show tortuous paths, sometimes with severe disturbances, as observable in intergranular mechanical fracture of Alumina.[10] Moreover, if the dielectric breakdown path preferentially takes place in the grain boundaries, where impurities and additives are concentrated, molten matter, expulsed from the breakdown channel because of the high pressure (see Fig. 7), should present a high concentration of these impurities and additives. This has been precisely verified using a chemical analysis (ESD).[7]

In single crystal Alumina (Sapphire), cleavage planes are clearly visible after dielectric breakdown tests. In Fig. 8, two cleavage planes *crossing* the dielectric breakdown channels can be observed. In Sapphire, the velocity of moving cracks on cleav-

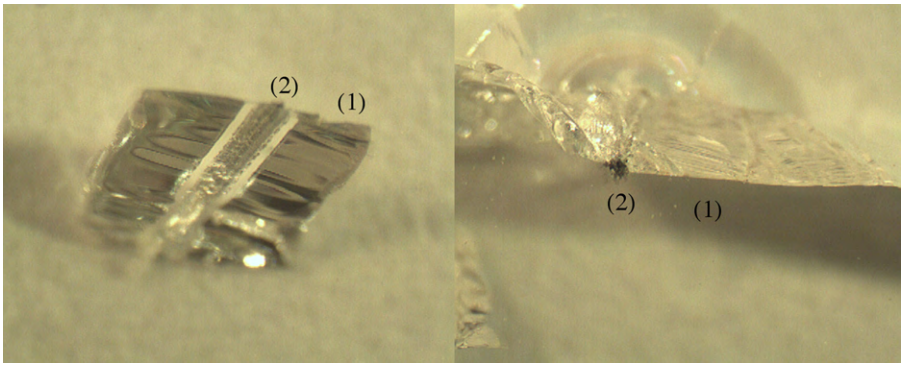

Fig. 8. Cleavage plane (1) and dielectric breakdown channel (2) in a Sapphire 2.54 mm-thick sample (Scanning Electron Micrograph). Left: cross-section view of a dielectric breakdown; right: top view of another dielectric breakdown.

Table 3
Relationship between toughness and dielectric strength of Sapphire and polycrystalline Alumina (dielectric strength: rms, RT, sine 50 Hz; $\partial V/\partial t = 1.6$ kV/s).

	Toughness (MPa $m^{1/2}$)	Dielectric strength (kV/mm)
Sapphire 2.54 mm-thick	3[a]	9.02
Alumina 99.5% 2.54 mm-thick	5[a]	11.37 (extrapolated from Fig. 2)

[a] Data from supplier.

age planes has been found to be higher than those obtained for polycrystalline Alumina.[11] Consequently, the corresponding toughness of Sapphire is lower than Alumina one. In Table 3, both toughness and dielectric strength of Sapphire and pure polycrystalline Alumina have been compared. As shown in this table, both mechanical and dielectric properties are in good agreement, i.e. the higher the toughness, the higher the dielectric strength, as previously shown with polycrystalline Alumina having different purities.

Another relationship between mechanical and dielectric strength of Alumina may be found in Ref.[2] In order to increase the mechanical strength of Alumina, zirconium dioxide has been added in Alumina powder before sintering. Alumina + ZrO_2 is indeed used in biomedical applications (prostheses) to increase (by a factor 1.5–2) the resistance to crack propagation.[12] The mechanical breakdown of Alumina occurs when an initial crack has been able to propagate through intergranular areas. At room temperature ZrO_2 has a monoclinic crystalline structure, whereas above 860 °C its structure is tetragonal. The transformation from tetragonal to monolitic structure induces a volume expansion. During sintering (about 1200 °C), Zirconium got a tetragonal phase. During the cooling process, Zirconium grains blocked between neighbouring Alumina grains cannot change from a tetragonal to a monoclinic phase. Nevertheless, under a mechanical load, if any crack tends to propagate through an intergranular path, voids between Alumina grains allow zirconium to change from a tetragonal to a monolitic structure. Then, the corresponding Zirconium volume expansion act as a 'crack blocker', increasing thus the mechanical strength of Alumina and particularly its resistance to crack growth. In the same time, the dielectric strength of such reinforced-Alumina has been increased, proving the relationship between their mechanical and dielectric behaviors.

4.2. Dielectric breakdown modelling

The experimental correlation between mechanical and dielectric strengths of Alumina being clearly demonstrated, the modelling of the dielectric breakdown is logically considered to be initiated by a mechanical fracture. Fracture mechanisms, leading to the concept of fracture toughness, have been firstly studied by Griffith,[13] whose works have inspired numerous researchers. Mechanical induced dielectric breakdown occurring during aging or during a dielectric strength test indicates that the mechanical breakdown takes place when the work done by the mechanical forces exceeds the crack propagation energy. In this breakdown modelling, the propagation of a mechanical crack is considered to be strongly dependent on the electric field at the tip of the crack. During aging (i.e. under a low applied field) the local electric field at the tip is reduced by the injected space charge (field limiting space charge). Consequently the crack propagates slowly from one electrode to the other one.[14] On the contrary, during dielectric breakdown test (i.e. when the applied voltage is continuously increasing)[15] and under special conditions (i.e. a little field moderation in particular regions of the sample), the energy for the formation and the propagation of the filamentary crack may be quickly reached. Indeed, under a high electric applied field, the charge injection is obviously higher than under a low applied field but injected charges get a higher mobility and the electric field at the tip is not as reduced as under low applied field.

In polycrystalline ceramic materials, we suggest that grain boundary regions may act as these particular regions. In that case, a high field may exist at the tip of the crack and one might expect carriers injection and impact-ionization phenomena during the crack propagation time. Impact-ionization induced luminescence might be recorded in order to verify such hypothesis. Nevertheless, if a crack propagates through the sample, fracto-emission (i.e. ejection of electrons and particles from cracks during fast fracture in brittle solids[9]) should also take place, leading to light emission as well.

In the case of elastic fracture under a constant mechanical load, a well known theory called *linear elastic fracture mechanism* has been developed.[9] The concept of fracture mechanics can also be applied to the problem of dielectric breakdown. An applied electric field will cause a dielectric breakdown while an applied mechanical load will causes a mechanical fracture. In both cases, the failure process may be connected to the presence of an initiating microcrack. The nature of the cohesive bonding between atoms in the ceramic material will define the resistance to the growth of this microcrack. Therefore, an analogous linear dielectric breakdown, based on a Griffith-like energy balance theory applied to a single conducting microcrack has been proposed.[16] The length of the initial defect from which the crack begins to grow is a crucial data.[17] Nevertheless, using the critical defect size obtained by mechanical tests does not provide a good agreement between measured and calculated dielectric breakdown fields.[18] Moreover, a recent experimental study has shown that the size of initial cracks existing at the sample surface do not affect the dielectric strength of Alumina.[19] These results clearly indicate that a simplified modelling cannot provide a satisfactorily result. However, post-mortem optical observations carried out on broken samples could provide useful information about the origin of the dielectric breakdown of Alumina and confirm that it is anyhow related to its mechanical properties.

4.3. Mechanical origin of the dielectric breakdown of Alumina

The crucial question to be solved consists in wondering if the observed craters detailed in Section 2 are generated when the dielectric breakdown takes place (i.e. they are induced by the breakdown) or if they are involved themselves in the breakdown

process (i.e. they may provide useful informations about the breakdown mechanism). As previously mentioned, the craters build up are not be attributed to any external energy release and has to be considered as originated from the breakdown mechanism itself. Then, one might expect that during the breakdown process, molten matter extracted from the breakdown channel is quickly cooled when reaching the insulating bath. That fast cooling may cause the fragmentation of the molten matter.[20] The impacts of fragmented matter could initiate cracks on the samples surface. These cracks may assist internal mechanical forces to release the stored electrostatic energy, leading to the craters build up. But, as clearly shown by optical observations, no molten matter trace was found on the surfaces of extracted matter from the craters: neither on not emptied craters (Fig. 6) or on pieces of matter originated from the craters area. Since molten matter may copiously be observed on the craters surfaces and not on the surface of matter extracted from them, one might assume that the explosive event leading to the craters build up occurs before the dielectric breakdown. In such hypothesis, the sizes of the resulting craters are then probably related to the dielectric breakdown mechanism and not randomly distributed. As suggested in Section 2, we consider in first approximation that the craters are supposed to have the shape of cones. A statistical analysis of the craters size has been performed in order to estimate if it obeys any law versus sample thickness. The craters diameters have been estimated on the sample surface, while the craters depths have been measured as follows. After breakdown, the neighbouring area of a crater gets weaker, allowing, by exerting a pressure in the middle of it, to break the sample in two parts. Sometimes, the mechanical rupture passes through the dielectric breakdown channel (as shown in Fig. 5), allowing the measurement of the crater depth. Crater diameter, depth and volume (mean values) of 96% polycrystalline Alumina have been reported in Fig. 9 versus samples thickness. As clearly shown in that figure, and in spite of the low accuracy in the crater depth estimation, the evolution of the craters sizes versus thickness is obviously not random: the higher the thickness, the higher the size of the crater. Moreover, the size of the crater is found to be nonlinear versus thickness: this can be associated with the size effect of ceramic material: the thinner samples show a tendency to greater mechanical strength. In other words, the size of the carter, in which mechanical forces act during the voltage application, can be related to the mechanical strength of the sample. This non-linearity is also found with Alumina dielectric strength, as indicated by the results of Fig. 2. Nevertheless, future investigations are necessary to complete that first correlation between mechanical and dielectric strengths. Among them, the estimation of the crater size versus Alumina purity, voltage rising rate and kind of electrodes should provide crucial information about the correlation between the extracted matter, related to the mechanical strength of Alumina, and its dielectric strength. Such investigations are actually in progress.

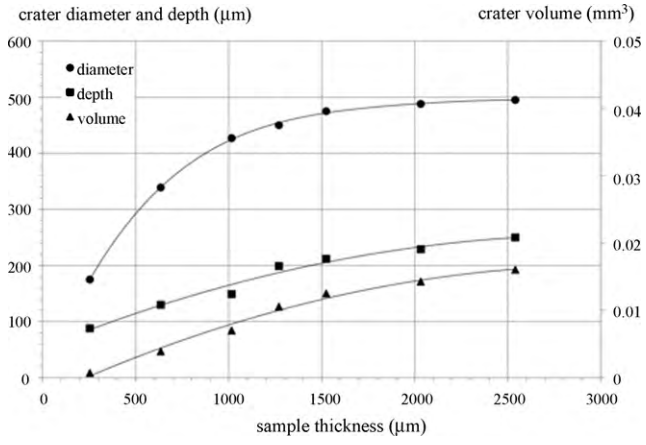

Fig. 9. Evolution of the craters sizes versus polycrystalline 96% Alumina sample thickness (RT, sine 50 Hz, plane–spherical electrodes, $\partial V/\partial t = 1.6$ kV/s).

5. Conclusions

The dielectric strength of polycrystalline α-Alumina samples having different thickness and purity has been measured. Whatever the thickness and the purity, craters have been observed at the vicinity of the breakdown channels. The mechanical origin of Alumina dielectric breakdown was often suggested to explain the presence of such carters. In order to provide new information supporting this assumption, optical observations of these dielectric breakdowns have been carefully performed. These observations have revealed that the size of 96% Alumina samples craters versus thickness is not random but follows a nonlinear evolution. Moreover, molten matter originated from the breakdown channels, has only been copiously observed on the craters surface, suggesting that the explosive event leading to the extraction of matter occurs before the dielectric breakdown. Finally, tortuous path and cleavage planes observed after dielectric breakdown respectively in polycrystalline and single crystal Alumina are in good agreement with mechanical cracks propagations occurring in such ceramic materials.

References

1. Miziolek AW, Palleschi V, Schechter I, editors. *Laser induced breakdown spectroscopy*. Cambridge, UK: Cambridge University Press; 2006.
2. Liebault J, Vallayer J, Goeuriot D, Treheux D, Thevenot F. How the trapping of charges can explain the dielectric performance of Alumina ceramics. *J Eur Ceram Soc* 2001;**21**:389–97.
3. Morse CT, Hill GJ. The electric strength of Alumina: the effect of porosity. *Proc Br Ceram Soc* 1970;**180**:23–5.
4. Owate IO, Freer R. Dielectric breakdown of ceramics and glass ceramics. In: *Proceeding of the 6th international conference on dielectric materials, measurements and applications*. 1992. p. 443–6.
5. Malec D, Bley V, Lebey T, Talbi F, Lalam F. Investigations on dielectric breakdown of ceramic materials. In: *Proceeding of the international conference on electrical insaulation and dielectric phenomena*. 2005. p. 63–6.
6. Yoshimura M, Bowen HK. Electrical breakdown of Alumina at high temperatures. *J Am Ceram Soc* 1981;**64**(7):404–10.
7. Owate IO, Freer R. AC breakdown characteristics of ceramic materials. *J Appl Phys* 1992;**72**:2418–22.
8. Dutarde E, Dinculescu S, Lebey T. On some electrical characteristics of AlN and Al_2O_3. In: *Proceeding of the International Symposium on Electrical Insulation*. 2000. p. 172–5.

9. Lawn B. *Fracture of brittle solids*. Cambridge University Press; 1993.
10. Swanson PL, Fairbanks CJ, Lawn BR, Mai YW, Hockey BJ. Crack-interface grain bridging as a fracture resistance I, mechanism in ceramics: I, experimental study on Alumina. *J Am Ceram Soc* 1987;**70**(4):279–89.
11. Sherman D, Be'ery I. Fracture mechanisms of sapphire under bending. *J Mater Sci* 2000;**35**(5):1283–93.
12. De Aza AH, Chevalier J, Fantozzi G, Schehl M, Torrecillas R. Crack growth resistance of Alumina, zirconia and zirconia toughened Alumina ceramics for joint prostheses. *Biomaterials* 2002;**23**(3):937–45.
13. Griffith AA. The phenomena of rupture and flow in solids. *Philos Trans R Soc Lond A* 1921;**221**(585–593):163–98.
14. Zeller HR, Schenider WR. Electrofracture mechanisms of dielectric aging. *J Appl Phys* 1984;**56**(2):455–9.
15. Fothergill JC. Filamentary electromechanical breakdown. *IEEE Trans Electr Insul* 1991;**26**(6):1124–9.
16. Garboszi EJ. Linear dielectric-breakdown electrostatics. *Phys Rev* 1988;**38**(13):9005–10.
17. Suo Z. Models for breakdown resistant dielectric and ferroelectric ceramics. *J Mech Phys Solids* 1993;**41**(7):1155–76.
18. Carabajar S, Olagnon C, Fantozzi G, Le Gressus C. Relations between electrical breakdown field and mechanical properties of ceramics. In: *Proceeding of the international conference on electrical insulation and dielectric phenomena*. 1995. p. 278–81.
19. Decup M, Malec D, Bley V. Impact of surface laser treatment on the dielectric strength of α-Alumina. *J Appl Phys* 2009;**106**(9):094103.1–4.
20. Jones H. Rapid solidification. In: *Monograph 8.* London, UK: Institute of Metals; 1982. p. 8–46.